Surface properties and biocompatibility of thick film materials used in ceramic bioreactors

Heike Bartsch[(1)]*, Ralf Peipmann[(1)], Marcel Himmerlich[(1)#], Marion Frant[(2)], Holger Rothe[(2)], Klaus Liefeith[(2)], Hartmut Witte[(1)]

1) Technische Universität Ilmenau, Institute of Micro- and Nanotechnologies MacroNano®, Gustav-Kirchhoff-Str. 7, 98693 Ilmenau, Germany
2) Institute for Bioprocessing an Analytical Measurement Techniques, Biomaterials Group, Rosenhof, 37308 Heilbad Heiligenstadt, Germany

* corresponding author

present address: European Organization for Nuclear Research CERN, CH-1211 GENEVA 23, Switzerland

Keywords: LTCC, thick film metallization, biocompatibility, surface properties, chemical composition, zeta potential

Abstract

Low temperature cofired ceramics (LTCC) have conquered a niche segment in biological microelectromechanical systems (BioMEMS) during the last two decades. Since 3-dimensional assembly and rapid prototyping capability are outstanding features of the technology, bioreactors with complex geometry can easily be produced. Particularly needed functions are working electrodes, e.g. for impedance measurements and reference electrodes consisting in platinum or silver-silver chloride. Although the distinct grainy surface of thick film materials influences the double layer properties, data describing the bioelectronic interface and biocompatibility of common thick film materials are rarely published up to now. This works aims to fill this gap by studying the surface properties, composition, electrochemical properties and biocompatibility of commercially available thick film materials. It was found that thick film gold is suitable as electrode material in direct cell contact since an appropriate proliferation of the cell culture was observed. Poly(3,4-ethylenedioxythiophene) coating decreases the absolute value of the zeta potential of thick film gold from 16.55 V to 11.78 mV without any change in vitality of the cells. Thick film platinum layers have a porous structure entailing an enlargement of the effective surface by a factor of 21.6 and can be used as reference instead of silver/silver chloride, which was identified to be incompatible with cell culture. The investigations show that some commercially available cost-effective thick film materials are compatible with cell culture and the here presented data give an orientation for the use of the same in LTCC bioreactors.

Introduction

Bioreactors must fulfill ambitious tasks, integrating various functions such as sensors for metabolism, signal capturing or actuation in one device [1]. The development of such complex systems needs platforms, which are capable to integrate different substrate technologies, reactions and operation conditions. Additionally, an easy plug-and-play use for the operator in the biolab must be guaranteed. Although the number of applications is low in comparison with numerous biologic microelectromechanical systems (BioMEMS) based on silicon and glass surface structuring, low temperature cofired ceramics (LTCC) is a promising niche technology on the bioreactor segment. Since

Preprints (www.preprints.org) | NOT PEER-REVIEWED | Posted: 18 January 2019 doi:10.20944/preprints201901.0185.v1

Peer-reviewed version available at *Materialia* **2019**; doi:10.1016/j.mtla.2019.100213

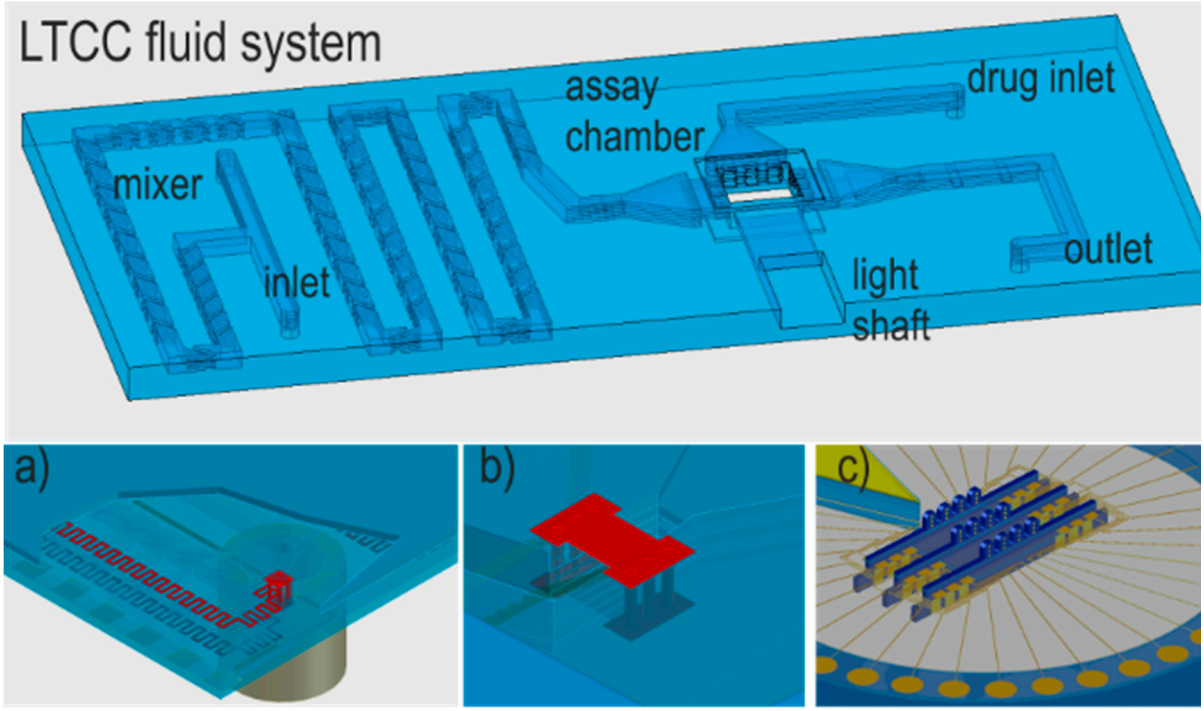

Figure 1: Example for a 3-dimensional LTCC bioreactor: a) integrated heater for temperature control; b) temperature sensor surrounding the channel; c) 3D-impedance electrodes, mounted through the glass bottom of the assay chamber.

the multilayer technology allows the design of complex fluidic systems [2-5], it offers a wide design spectrum for the production of 3-dimensional systems. Figure 1 depicts examples for complex ceramic fluid model system.

A wide portfolio of LTCC materials is available for tailored applications [6] and customized, biocompatible tapes can already be produced [7]. Commercially available LTCC materials offer manifold opportunities for sensor integration [8], allowing temperature control [9,10] and flow rate measurement [11] in microreactors, guaranteeing thus stable operation conditions. Sensor principles based on LTCC technology are available for the detection of metabolic products [12], oxygen [13], pH-values [14] and chemical species [3,15-16]. Optical interfaces [5,17] and the integration of potentiometric sensors [18-19], impedance sensors [20] and even CMOS-chips [21,22] allow the reliable control of cell cultures.

Green Tape™ 951 (DuPont Nemours) is widely used for rapid prototyping of fluid reactors. Although the material is not intended for such applications, studies revealed that the fired base ceramic is compatible with mammalian cell cultures [11,21]. However, thick film metallization made of available pastes have shown inconsistent results. Therefore, this study aims to characterize and evaluate thick film layers based on different pastes of the 951™ product family. Gold electrodes are widely used as impedance electrodes. In principle, the thick film gold composition 5740A is suitable for the establishment of such electrodes. The paste 9696R is tested to evaluate the possibility of platinum electrode integration into bioreactors. Silver / silver chloride (Ag/AgCl) reference electrodes based on the paste 6145R and thick film gold electrodes, electro-polymerized with poly(3,4-ethylenedioxythiophene) (PEDOT), complete the material selection of this study, which pursues the systematic quantification of crucial performance characteristics for the use of such thick film materials in fluid analytics. Surface topography, composition, Zeta potential and biocompatibility are investigated with the goal to provide an orientation for the use of different electrode materials in complex systems based on the versatile multilayer ceramic technology.

Materials, methods and results

LTCC sample preparation

The samples have a round shape with a diameter of 15 mm, which fits optimally in a 24-well-plate. Nine round blanks are situated on one LTCC substrate (see Figure 2). It consists of four tape layers. The contour of the round blanks is laser cut in the green state. Bars connect the single round blanks with the substrate in order to connect it electrically for electrochemical treatments and assure mechanical stability. After processing, these bars can be cut with a wafer dicing machine and thus the round blanks are separated for further testing.

Thick film layer, covering almost the whole area of the round blanks, are screen printed with the respective paste on top the uppermost green sheet (screen with 325-mesh stainless steel fabric and 15-µm emulsion layer thickness). The printing setup was squeegee 85° shore (length 100mm and angle 45°), squeegee velocity 50 mm/s and an applied squeegee force of 50 N. The take-off depends on the paste. It amounts to 1.2 mm for the silver composition and to 1.0 mm for gold and platinum. The green sheets are laminated at 70°C for 10 minutes at a pressure of 200 bar (IL-4008 Isostatic Laminator, Pacific Trinetics Corporation, Los Alamitos, California). The laminated substrates sinter in a fast ramping furnace (PEO-603, ATV Technologie GmbH, Germany). The heating rate is 10 K/min in the beginning of the procedure and reduces to 1 K/min between 400°C and 500°C during debindering. A fast heating period with 10 K/min up to 820°C follows, then the rate is decreased to 2.75 K/min between 820°C and the final sinter plateau at 875°C which is held for 30 min. The cool-down starts at 7 K/min to 700°C and is beyond reduced to 5 K/min (500°C) and 4 K/min (400°C). Below this temperature, the rate is 3.3 K/min. The thick films on top of these samples have a thickness of 5 µm, approximately. The samples prepared with thick film gold are labeled as Au and those with platinum with Pt in this work.

After LTCC processing, the silver thick films are anodized at 1.9 A/dm² for 2 min in a beaker with 1 molar aqueous solution of hydrochloric acid (HCl). These samples are labeled as Ag/AgCl in the following.

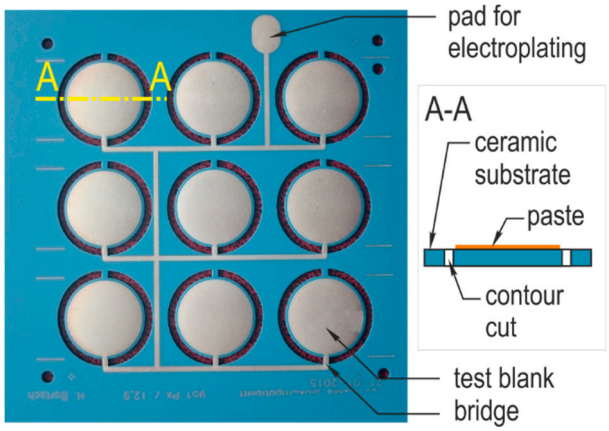

Figure 2: LTCC substrate with screen printed round blanks, used as samples.

The reference potential of these thick film-based Ag/AgCl reference electrodes is measured against an Ag/AgCl (saturated KCl) electrode using 8 independently anodized samples. The median value of the measured potential is 67.0 mV and the average value is 67.1 mV. The 25 / 75 percent quantiles are 65.5 / 72.0 mV, respectively.

A PEDOT layer was deposited on four substrates prepared with thick film gold. A solution of 10 mmol/l 3,4-ethylenedioxythiophene (EDOT) 97% (Sigma Aldrich) is dissolved in a 0.5 molar aqueous solution of sulphuric acid. Thereafter 34 mmol/l sodium dodecyl sulfate (SDS) are added as wetting agent. After

Preprints (www.preprints.org) | NOT PEER-REVIEWED | Posted: 18 January 2019 doi:10.20944/preprints201901.0185.v1

Peer-reviewed version available at Materialia 2019; doi:10.1016/j.mtla.2019.100213

mixing, the electrolyte is leave to stand for 24 h at 8°C to allow conditioning. The electro-polymerization is carried out at a constant voltage of 0.9 V for three minutes with a platinum grid serving as counter electrode. The samples are labeled as PEDOT in the following.

Surface characterization using laser scanning microscopy (LSM) and scanning electron microscope (SEM), X-ray photoelectron spectroscopy (XPS) analysis, biocompatibility tests and zeta potential measurements are carried out on the separated round blanks, either diced or broken out of the carrier substrate.

Surface roughness

The surface was captured with a laser scanning microscope (LSM, OLS 4100, Olympus, Germany). The scanned area is 128 µm x 128 µm and the lateral resolution amounts to 200 nm. The data were analyzed using the software MoutainsMap. Invalid data points due to insufficient reflection on steep edges are removed and equalized and the sample surface is leveled along a linear regression plane. A Gaussian filter (ISO 166 10-61) with a cut-off wave length of 8 µm is applied. Surface waviness and roughness are analyzed according to ISO 25178. The roughness differs strongly dependent on the thick film material. Figure 3 depicts the area roughness parameters arithmetical mean height (Sa), root mean square height (Sq) and maximum height (Sz), evaluating the whole area of 128 µm x 128 µm. Figure 4 gathers the true color images and topography profiles of the LSM scans. The waviness amounts to 0.62 µm ± 0.02 µm for all investigated surfaces and is supposed to have its origin in the screen structure. The screen emulsion thickness and wire diameter are expected to be important process parameter for the resulting waviness. Traces of the screen mesh can be identified as rectangular depression pattern in Figure 4 f,d. On the other samples, such traces are probably leveled during lamination. The surface parameters Sa and Sq quantify grain structure and porosity.

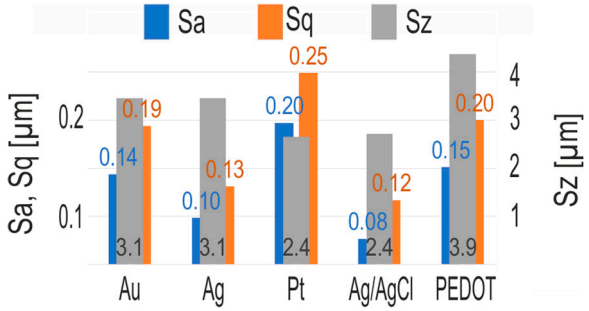

Figure 3: Surface roughness parameter Sa, Sq and Sz of thick film based surfaces in accordance with ISO 25178 (cut-off length 8 µm).

Surface enlargement

The x-y-z surface data were exported as a binary stereolithography file (STL file format). This point coordinates are imported in ANSYS Space Claim 18.2 (ASC). The software generates a triangulated model of the real measured surface and the calculation of its surface area is possible using the mass property tool. In this way, the estimation of the real surface area, taking the roughness into account, is possible. The surface enlargement can be estimated, relating the value of the software calculation with that of the projection area of 128x128 µm². The results of this procedure are summarized in Table 1.

Table 1: Surface enlargement due to surface roughness, compared with a flat projection area of the same footprint

Material	Calculated area [µm²]	Projection area [µm²]	Ratio	Surface enlarge. [%]
Au	17602	16384	1.074	7.4
Pt	19916	16384	1.216	21.6
Ag/AgCl	16933	16384	1.033	3.3
PEDOT	17885	16384	1.092	9.2

Topography

Obviously, the height range is similar for all materials. The height distribution of the surfaces varies only slightly. However, the roughness of the different materials varies. Gold and PEDOT samples have a similar surface structure, while a fine-grained surface texture is observed on the platinum surface. On the other hand, silver chloride layers exhibit large even regions. The true color image of the PEDOT surface in Figure 4g reveals through-shining gold areas. Here, the PEDOT layer is either very thin, or the electropolymerized layer is not fully oxidized and therefore appears transparent.

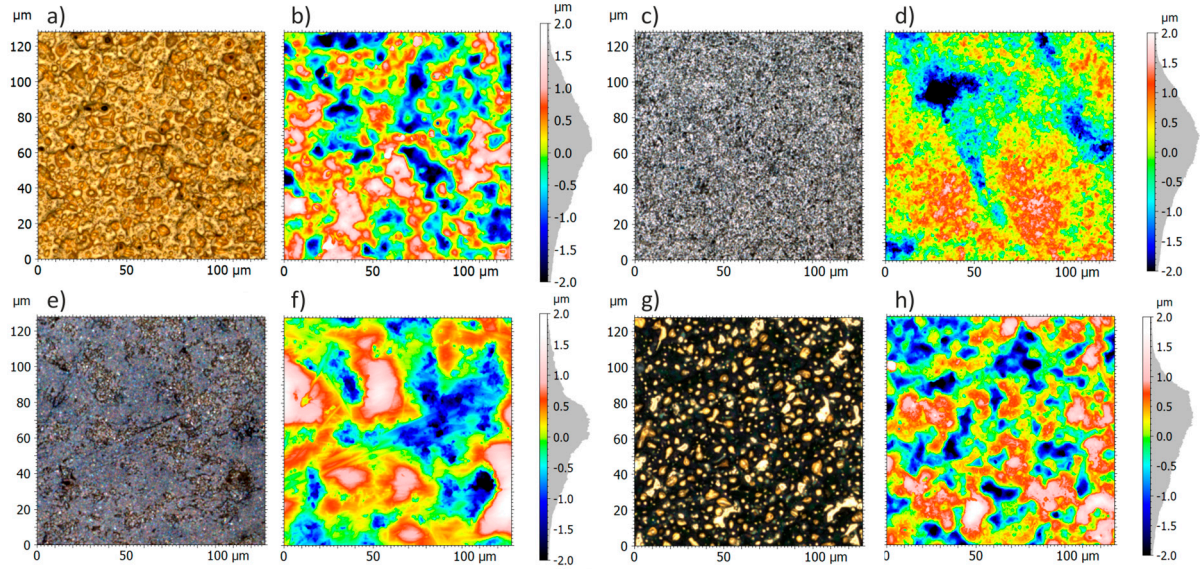

Figure 4: LSM images of the different thick film surfaces, either true color and height profile with histogram; a, b) gold; c,d) platinum; e,f) Ag/AgCl; g,h) PEDOT

SEM

The surfaces of all samples that were initially characterized by XPS (see below) were also investigated by SEM (Hitachi 4800) by clamping them onto a substrate holder and loading them into the vacuum system. The surface investigation was carried out under a tilt of 7° with respect to the surface normal at a working distance of 8 mm (acceleration voltage 15 kV / 10 µA for metallic samples and 2 kV / 2 µA for PEDOT and Ag/AgCl). The surfaces were investigated using the topography contrast and material contrast to localize areas of different composition. The magnitude was 2000x or 1000x, dependent on the surface structure. The SEM micrographs are depicted in Figure 5.

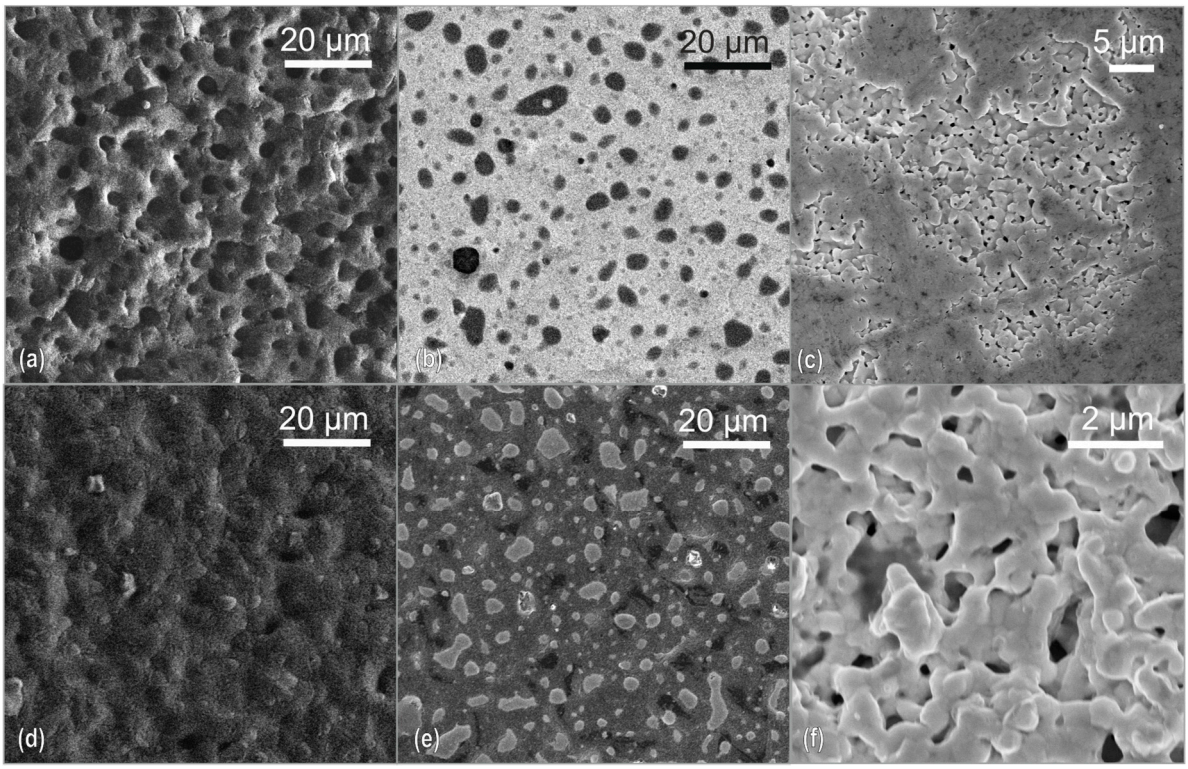

Figure 5: SEM micrographs of different thick film surfaces: a) topography contrast image of thick film gold and b) material contrast of the same; c) Ag/AgCl surface with porous region; d) topography contrast of PEDOT surface and e) material contrast of the same; f) porous structure of the platinum surface.

Surface composition

The respective layer´s surface composition was investigated using XPS in an experimental setup described in detail in [23]. Measurements were performed on as loaded samples in normal emission geometry using a spot size of 1 mm in diameter and a typical depth of information of 5-7 nm for inorganic material and 7-10 nm for organic films. Metallic surfaces (gold, platinum) and Ag/AgCl samples were bombarded by Ar^+ ions (3 keV) to remove adsorbates and the first near-surface layers. Due to the rough topography and the partially porous surface structure of the different layers, the ion-based technique is not as effective to clean the surface as for flat surfaces resulting in different sputtering rates for different regions. PEDOT samples were not ion-treated due to their low film thickness and to avoid fragmentation of the polymer film which falsifies surface analysis of organic layer.

Table 2 summarizes the results of a quantitative elemental analysis for the metal-based layers. The metallic thick films consist to a great extent of their respective metal elements. Different metal oxides, added as glass formers to ensure reliable adhesion on the ceramic substrate, are present and identified within the measurements. All samples have hydrocarbon and oxide-based surface adsorbates. The amount of these species reduces after sputtering, but does not vanish. Plasticizers and binder residues, which condense during sintering in the cooling phase or readsorb at the surface, are assumed to be the origin.

The platinum layer (paste 9698) includes a low content of lead. Mn, Co and traces of P and Zn indicate the presence of a mixture of various glass formers acting as sinter additives. The gold layer (paste 5740A) contains exclusively lead glass in low concentration. Traces of iodine and chlorine were detected in this case as well. These are assigned to originate from the gold powder processing, where halogen-based solutions (e.g. aqua regia or potassium iodide) are used to dissolve the bulk metal and particles are subsequently precipitated.

Preprints (www.preprints.org) | NOT PEER-REVIEWED | Posted: 18 January 2019 doi:10.20944/preprints201901.0185.v1

Peer-reviewed version available at Materialia 2019; doi:10.1016/j.mtla.2019.100213

The Ag/AgCl layers exhibit an almost stoichiometric Ag:Cl ratio at the surface. Only traces of oxide-bound lead were found. After ion bombardment, the Ag:Cl ratio increases. This effect could either indicate the existence of a transition zone between the anodized surface and the silver bulk region or an artifact due to preferential sputtering of light Cl atoms from the surface. Nitrogen is detected on the untreated surface and its content decreases close to the detection limit in the bulk region.

The excess carbon is caused by surface adsorbates, which are supposed to originate from the sinter process. The volatile organics remain in the furnace oven atmosphere and readsorb at the surface. A surface modification by plasma treatment, bake out or suitable solvent cleaning procedures could minimize the amount of surface impurities.

Table 2: Surface composition (at. %) extracted from XPS measurements of the different metal- based thick films.

Material *Treatment*	Carbon	Mayor elements	Lead (oxide-bound)	Other constituents*
Pt	42.5	Pt: 21.3	1.0	Mn: 3.8 / Co: 1.3 / P: 0.5/ Zn: 0.4
as loaded				
sputtered	11.6	Pt: 73.0	0.2	Mn: 3.6 / Co: 0.2 / P<0.1/ Zn<0.1
Au	25.6	Au: 35.3	1.7	Cl: 0.3 / I: 0.3
as loaded				
sputtered	8.1	Au: 67.3	1.8	Cl: 0.1 / I: <0.1
Ag/AgCl	40.2	Ag: 20.5	0.1	N: 4.5
as loaded		Cl: 21		
sputtered	11.7	Ag: 49.5 Cl: 38.3	0.1	N: <0.1

For chemical analysis of the electro-polymerized films, samples were immediately broken out of the batch after deposition and transferred through the ambient within 30 min to insert them into the high vacuum system for XPS. From quantitative analysis of the obtained core level spectra, the elemental C : O : S ratio of the electropolymerized PEDOT film on thick film golf was estimated to be 7.8 : 3.6 : 1 (nominal molecular ratio 6 : 2 : 1), assuming a homogeneous elemental distribution in a simple quantification model. There is no substrate related gold signal detected, indicating the formation of a dense and compact PEDOT layer that homogeneously covers the underlying Au/LTCC structure. The spectral characteristics of the oxygen, carbon and sulphur core levels (not shown) are in very good agreement with earlier reports of XPS analyses of electropolymerized PEDOT films [24], [25].

Zeta potential measurement

Zeta potential (surface charge) measurements on the planar surfaces are carried out with an electro-kinetic analyzer (SurPASS, Anton Paar GmbH, Ostfildern, Germany). A reference electrolyte with a concentration of 1 mmol/l potassium chloride (KCl) is conducted through a defined measurement channel with a width of 110-120 µm, which is adjusted between two clamped test blanks. After filling the assembly with the electrolyte, the pressure is increased following a defined ramp up to 30´000 Pa. The resulting flow carries away the outer ions and causes thus a potential difference. Zetapotential calculation was performed according to equation 1:

$$\zeta = \frac{\eta \kappa_{sp}}{\varepsilon \varepsilon_0} \frac{d\Psi}{dp} \qquad (1)$$

ζ	*zeta potential*	*[mV]*	Ψ	*electrical potential*	*[mV]*
η	*viscosity*	*[Pas]*	κ_{sp}	*specific conductivity*	*[S/m]*
ε	*permittivity*	*[As/Vm]*	p	*pressure*	*[Pa]*

The data are evaluated applying the method of Fairbrother and Mastin [26]. The surface conductivity was corrected by a reference measurement using 0.1 molar aqueous solution of KCl. Firstly, point

Preprints (www.preprints.org) | NOT PEER-REVIEWED | Posted: 18 January 2019 doi:10.20944/preprints201901.0185.v1

Peer-reviewed version available at Materialia 2019; doi:10.1016/j.mtla.2019.100213

measurements were carried out at constant pH 6 by means of a value range of four for each material. After each measurement, the chamber was cleaned with distilled water. Figure 6 a) depicts the measured values. Figure 6 b) presents the resulting course of the zeta potential dependent on pH. The isoelectric point (IEP) was determined by titration measurements, repeated twice for each material. The mean of the IEP amounts to 0 for Ag/AgCl, 2.7 for Pt, 3.1 for Au and 3.8 for PEDOT.

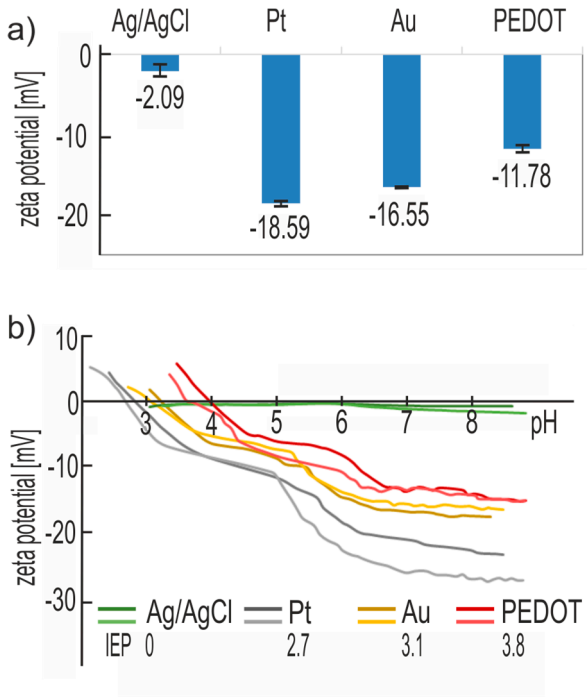

Figure 6: Measurement results of electro-kinetic analysis. a) zeta potential at pH 6; b) zeta-potential curves as a function of pH.

The zeta potential measurements at constant pH value reveal a good reproducibility. The titration course differs between the single measurements for Pt and PEDOT samples, possibly due to differences in surface topography or an inhomogeneous surface chemistry. Curves of Au and Ag/AgCl samples have only marginal deviations.

Biocompatibility test

The biocompatibility was evaluated following the norm "Biological assessment of medical devices" DIN EN ISO 10993-5. The cell line MC3T3-E1 (osteoblast, mouse C57BL/6 calvaria) was used in a cell culture using alpha medium (AlphaMEM) with 10 % fetal bovine serum (FBS) and 1 % penicillin-streptomycin (PenStrep).

All samples were autoclaved first, with exception of PEDOT coated thick film gold. These ones were sterilized with ethanol. At the round samples placed in 24-well plates 20´000 cell per cm² were seeded. As reference tissue culture material served a commercial well plate made off polystyrene (TCPS). The culture time was 3 days and three independent trials are carried out. After incubation, three samples of each materials were used for cell counting, based on fluorescence microscopy. Vitality and cell proliferation were determined after 3 days. Further, three more samples served for metabolic testing using (2,3-bis-(2-methoxy-4-nitro-5-sulfophenyl)-2H-tetrazolium-5-carboxanilide (XTT) in order to examine the activity of the mitochondrial dehydrogenase. Respectively, one sample of trial 1 and 3 was prepared for confocal laser scanning microscope (CLSM, Zeiss Germany, LSM 710) analysis with actin and cell core coloration. The results of the cell counting, vitality and XTT activity are depicted in Figure 7. CLSM images are depicted in Figure 8.

Preprints (www.preprints.org) | NOT PEER-REVIEWED | Posted: 18 January 2019 doi:10.20944/preprints201901.0185.v1

Peer-reviewed version available at Materialia 2019; doi:10.1016/j.mtla.2019.100213

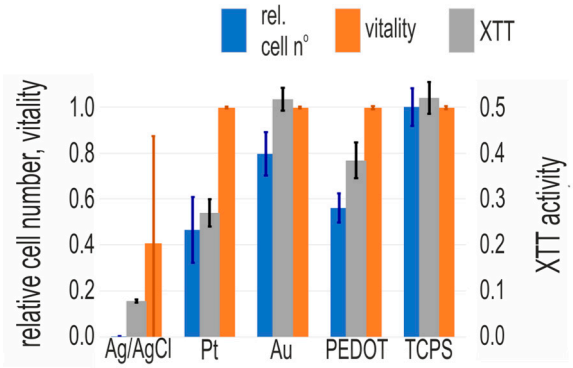

Figure 7: Cell number, vitality and XTT activity of the investigated thick film materials

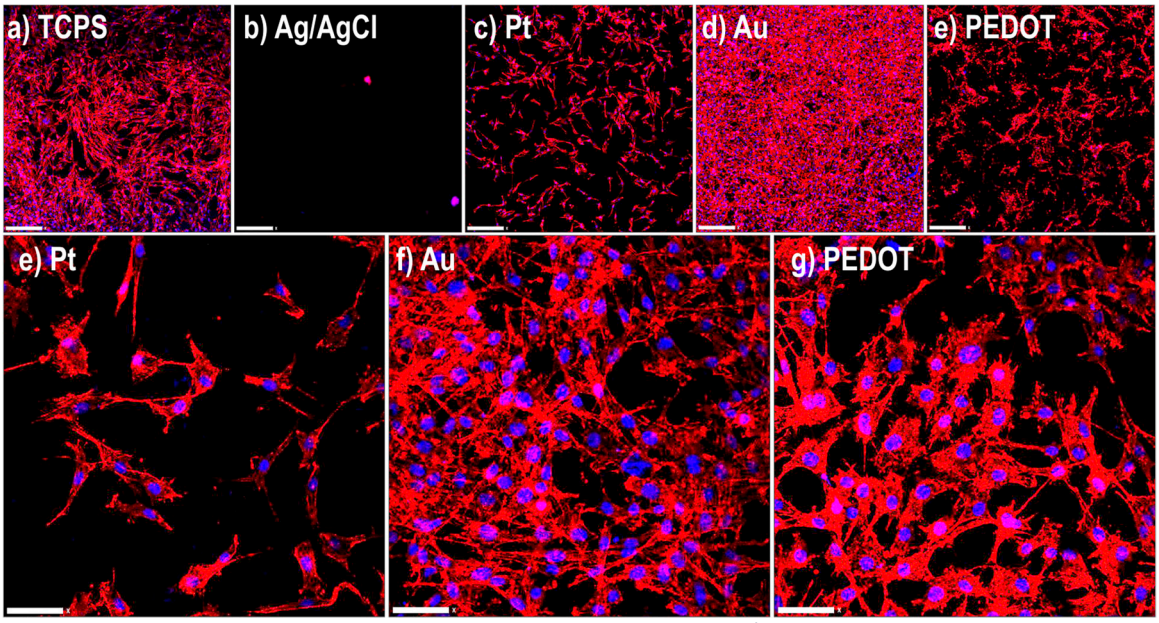

Figure 8: CLSM images of cells on different surfaces: a) TCPS reference; b) Ag/AgCl; c,e) Pt; d,f) Au and e,g) PEDOT.

The results of cell counting, XTT test (in vitro) and fluorescence microscope evaluation reveal significant differences in biocompatibility of the different surfaces. The cell compatibility of thick film gold (Au) is comparable with this of the TCPS reference. Cells grow in high number, spread well across the surface and show high vitality and enzymatic activity as well. Deposition of PEDOT layers on this surface leads to reduced cell proliferation, cell number and cell spreading decrease, but vitality and XTT activity are obviously not affected. Pt layers based on paste 9896R cause a significant reduction of the cell proliferation maintaining high vitality at the same time. CLSM images confirm this aspect, revealing well spread, but few osteoblasts. The anodized thick film silver layer (Ag/AgCl) is incompatible with biologic treatments. We observed only few inactive cells and a more or less round phenotype was visible in the CLSM images.

Discussion and conclusion

The surface roughness of thick film gold layers based on the paste 5740A entails a moderate surface enlargement. SEM investigations and XPS analysis allow the conclusion, that glass frit grains (Figure 5a, b) are present at the surface. XTT activity and vitality are excellent, revealing that the material does not harm living cells in direct contact. The used cell cultures have shown an appropriate proliferation. Consequently, the thick film material is suitable for use as interface materials for electrodes in in vitro cell cultures, for example as impedance electrode. An emerging application of such electrodes is the

use in 3-dimensional cell cultures for recordings of electroactivity, which already was proven with primary rat hippocampal and cortical cell cultures over a period of 6 weeks [20].

The Pt layers based on paste 9698 show the highest roughness. The surface structure results in a high surface enlargement. Since the calculation method for the real surface does not represent undercut structures, the real active surface is expected to be even larger. Therefore, the surface provides a large area for the adhesion of adsorbates, which is visible in the high carbon content measured by XPS analysis. The pore size of the platinum layer is in the range between 50 nm and 1 µm. However, the surface structure has no negative effect on the cell spreading behavior over the surface. The XPS analysis revealed oxidic bound Pb, Mn, Co and traces of P and Zn, which most likely have their origin in the glass component of the paste. In contrast to electroplated platinum black, which contains traces of metallic lead from the electrolyte [27], the material can be rated as non-cytotoxic, since the vitality of the cells was high and the cells spread well across the surface. The lower cell proliferation could be a consequence of the used glass; it turned out that some glass compositions are incompatible with mammalian cell lines [11]. Hydrocarbon surface adsorbates, which have an especially high concentration at the porous platinum surface, can be a further factor. An adequate cleaning protocol could possibly overcome this disadvantage. In addition to these factors, platinum showed the most negatively charged surface associated with the greatest environmental pH dependency. Both can also affect the cell-compatible properties. Nonetheless, sensor applications can benefit from the particular surface structure. Glucose sensors take advantage of surface enlargement, because porosity causes an increase of the current response [28-29]. Surface enlargement entails also higher impedance sensitivity [30]. Platinum can also serve as a reference electrode. Recently published studies indicate that platinum electrodes could substitute classical Ag/AgCl or calomel electrodes, when the working conditions prohibit its use due to different reasons [31]. Thick film platinum layers are hence applicable as counter electrodes, reference electrodes or as glucose and impedance sensing electrodes in cell culture devices. However, the material should not be directly used in the culture chamber to guarantee an undisturbed cell growth.

The anodization of thick film silver produced Ag/AgCl layers led to a significant decrease in Sz. The Silver/silver-chloride surface exhibits a likewise high carbon content. This fact neither correlates with the roughness, nor with surface enlargement. The SEM image in Figure 5 c reveals fine-porous regions, which would cause a surface enlargement, but cannot be recognized by LSM. Adhesion of surface adsorbates in these pores could explain the larger carbon content revealed by XPS measurement. The potential against a standard Ag/AgCl electrode was 67 mV. A possible reason for this deviation could be the depletion of chloride ions. The surface has a very low zeta potential value. Since cell proliferation, XTT activity and vitality are low, the material must be rated as non-biocompatible. In bioreactors, platinum reference electrodes should be used instead.

The deposition of PEDOT on thick film gold causes a higher interface roughness. Through-shining spots visible in the true color image Figure 4g) could indicate incomplete coverage but the SEM image in Figure 5d) reveals a closed layer morphology. Since there was no underlying gold detected by XPS analysis, the electropolymerized film is assumed to be dense. The spots might have its origin in varying composition or thickness. The material contrast image in Figure 5 e) unveils bright spots, where radiation penetrates the probably locally thinner PEDOT layer. Here, the direct comparison with the topography image 5d) captured on the same picture section, leads to the conclusion that the layer is dense but varies in thickness.

PEDOT coating decreases the absolute value of zeta potential in comparison with thick film gold. The isoelectric point is the highest value in the study. Despite the fact, that XTT activity and proliferation are lower than that on pristine thick film gold, the vitality was proven to be excellent. PEDOT functionalization can thus be rated as biocompatible. The conducting polymer is suitable for

investigations of electroactive cell cultures [32], e.g. by means of neuronal microelectrode assays [33] and for impedance-based proliferation sensors [34,35].

The present study has shown that cost-effective thick film technology can produce biocompatible electronic interfaces, which are easily integrable in bioreactors based on LTCC technology. Expanding the diversity of feasible designs to 3-dimensional assemblies, this integration enables the implementation of innovative fluid devices.

Acknowledgement

This work was supported by the Carl Zeiss Foundation (grant 0563-2.8/399/1 and 0563-2.8/416/3). We are grateful for financial support by the State of Thuringia and the European Union (ESF and ERDF) under Grant 12021–715.

Declaration of interest statement

The authors certify that they have no affiliations with or involvement in any organization or entity with any financial interest or non-financial interest in the subject matter or materials discussed in this manuscript.

References

[1] H. Witte, C. Schilling, The Concept of Biomechatronic Systems as a Means to Support the Development of Biosensors, Int J Biosen Bioelectron 2 (4) (2017) 114-115.

[2] N. Ibáñez-García, J. Alonso, C.S. Martínez-Cisneros, F. Valdés, Green-tape ceramics. New technological approach for integrating electronics and fluidics in microsystems, TrAC Trends in Analytical Chemistry 27 (1) (2008) 24–33.

[3] A. Vasudev, A. Kaushik, Y. Tomizawa, N. Norena, S. Bhansali, An LTCC-based microfluidic system for label-free, electrochemical detection of cortisol, Sensors and Actuators B: Chemical 182 (2013) 139–146.

[4] N. Halonen, J. Kilpijärvi, M. Sobocinski, T. Datta-Chaudhuri, A. Hassinen, S.B. Prakash, P. Möller, P. Abshire, S. Kellokumpu, A. Lloyd Spetz, Low temperature co-fired ceramic packaging of CMOS capacitive sensor chip towards cell viability monitoring, Beilstein journal of nanotechnology 7 (2016) 1871–1877.

[5] K. Malecha, Low temperature co-fired ceramics based modular fluidic system for efficient optical measurements, Int J Appl Ceram Technol 14 (4) (2017) 630–635.

[6] M.T. Sebastian, H. Jantunen, Low loss dielectric materials for LTCC applications: A review, International Materials Reviews 53 (2) (2013) 57–90.

[7] J. Luo, R.E. Eitel, A Biocompatible Low Temperature Co-fired Ceramic Substrate for Biosensors, Int J Appl Ceram Technol 11 (3) (2014) 436–442.

[8] D. Jurków, T. Maeder, A. Dąbrowski, M.S. Zarnik, D. Belavič, H. Bartsch, J. Müller, Overview on low temperature co-fired ceramic sensors, Sensors and Actuators A: Physical 233 (2015) 125–146.

[9] C.S. Martínez-Cisneros, N. Ibáñez-García, F. Valdés, J. Alonso, LTCC microflow analyzers with monolithic integration of thermal control, Sensors and Actuators A: Physical 138 (1) (2007) 63–70.

[10] H. Bartsch, T. Welker, K. Welker, H. Witte, J. Müller, LTCC based bioreactors for cell cultivation, IOP Conf Ser Mater Sci Eng 104 (2016) 12001.

[11] H. Bartsch de Torres, C. Rensch, M. Fischer, A. Schober, M. Hoffmann, J. Müller, Thick film flow sensor for biological microsystems, Sensors and Actuators A: Physical 160 (1-2) (2010) 109–115.

[12] P. Ciosek, K. Zawadzki, J. Łopacińska, M. Skolimowski, P. Bembnowicz, L.J. Golonka, Z. Brzózka, W. Wróblewski, Monitoring of cell cultures with LTCC microelectrode array, Analytical and bioanalytical chemistry 393 (8) (2009) 2029–2038.

[13] J. Luo, T. Dziubla, R. Eitel, A low temperature co-fired ceramic based microfluidic Clark-type oxygen sensor for real-time oxygen sensing, Sensors and Actuators B: Chemical 240 (2017) 392–397.

[14] L. Manjakkal, B. Synkiewicz, K. Zaraska, K. Cvejin, J. Kulawik, D. Szwagierczak, Development and characterization of miniaturized LTCC pH sensors with RuO 2 based sensing electrodes, Sensors and Actuators B: Chemical 223 (2016) 641–649.

[15] M.R. Gongora-Rubio, M.B. Fontes, Z.M. da Rocha, E.M. Richter, L. Angnes, LTCC manifold for heavy metal detection system in biomedical and environmental fluids, Sensors and Actuators B: Chemical 103 (1-2) (2004) 468–473.

[16] N. Ibañez-Garcia, R.M. Gonçalves, Z.M. da Rocha, M.R. Góngora-Rubio, A.C. Seabra, J.A. Chamarro, LTCC meso-analytical system for chloride ion determination in drinking waters, Sensors and Actuators B: Chemical 118 (1-2) (2006) 67–72.

[17] T. Welker, T. Geiling, H. Bartsch, J. Müller, Design and Fabrication of Transparent and Gas-Tight Optical Windows in Low-Temperature Co-Fired Ceramics, Int J Applied Ceramic Technology 10 (3) (2013) 405–412.

[18] P. Ciosek, W. Wróblewski, Potentiometric electronic tongues for foodstuff and biosample recognition--an overview, Sensors 11 (5) (2011) 4688–4701.

[19] Almeida, S A A, E. Arasa, M. Puyol, C.S. Martinez-Cisneros, J. Alonso-Chamarro, Montenegro, M C B S M, Sales, M G F, Novel LTCC-potentiometric microfluidic device for biparametric analysis of

organic compounds carrying plastic antibodies as ionophores: application to sulfamethoxazole and trimethoprim, Biosensors & bioelectronics 30 (1) (2011) 197–203.

[20] H. Bartsch, M. Himmerlich, M. Fischer, L. Demkó, J. Hyttinen, A. Schober, LTCC-Based Multi-Electrode Arrays for 3D in Vitro Cell Cultures, J Ceram Sci Tech 06 (04) (2015) 315–324.

[21] N. Halonen, J. Kilpijärvi, M. Sobocinski, T. Datta-Chaudhuri, A. Hassinen, S.B. Prakash, P. Möller, P. Abshire, E. Smela, S. Kellokumpu, A.L. Spetz, Low Temperature Co-fired Ceramic Package for Lab-on-CMOS Applied in Cell Viability Monitoring, Procedia Engineering 120 (2015) 1079–1082.

[22] J. Kilpijärvi, N. Halonen, M. Sobocinski, A. Hassinen, B. Senevirathna, K. Uvdal, P. Abshire, E. Smela, S. Kellokumpu, J. Juuti, A. Lloyd Spetz, LTCC Packaged Ring Oscillator Based Sensor for Evaluation of Cell Proliferation, Sensors 18 (10) (2018) 3346.

[23] C.A. Vlaic, S. Ivanov, R. Peipmann, A. Eisenhardt, M. Himmerlich, S. Krischok, A. Bund, Electrochemical lithiation of thin silicon based layers potentiostatically deposited from ionic liquid, Electrochimica Acta 168 (2015) 403–413.

[24] S.A. Spanninga, D.C. Martin, Z. Chen, X-ray Photoelectron Spectroscopy Study of Counterion Incorporation in Poly(3,4-ethylenedioxythiophene), The Journal of Physical Chemistry C 113 (14) (2009) 5585–5592.

[25] S.A. Spanninga, D.C. Martin, Z. Chen, X-ray photoelectron spectroscopy study of counterion incorporation in poly(3,4-ethylenedioxythiophene) (PEDOT) 2: Polyanion effect, toluenesulfonate, and small anions, The Journal of Physical Chemistry C 114 (35) (2010) 14992–14997.

[26] F. Fairbrother, H. Mastin, CCCXII.—Studies in electro-endosmosis. Part I, J Chem Soc, Trans 125 (0) (1924) 2319–2330.

[27] M. Schuettler, T. Dorge, S. Wien, S. Becker, A. Staiger, M. Hanauer, S. Kammer, T. Stieglitz, Cytotoxicity of Platinum Black, in: M.T. Shaw, W.J. MacKnight (Eds.), Proceedings of the 10th Annual Conference of the International FES Society, July 2005 – Montreal, Canada, John Wiley & Sons, Inc, Hoboken, NJ, USA, 2005, pp. 1–6.

[28] S. Gu, Y. Lu, Y. Ding, L. Li, H. Song, J. Wang, Q. Wu, A droplet-based microfluidic electrochemical sensor using platinum-black microelectrode and its application in high sensitive glucose sensing, Biosensors & bioelectronics 55 (2014) 106–112.

[29] H.-K. Seo, D.-J. Park, J.-Y. Park, Fabrication and characterization of platinum black and mesoporous platinum electrodes for in-vivo and continuously monitoring electrochemical sensor applications, Thin Solid Films 516 (16) (2008) 5227–5230.

[30] C. Boehler, T. Stieglitz, M. Asplund, Nanostructured platinum grass enables superior impedance reduction for neural microelectrodes, Biomaterials 67 (2015) 346–353.

[31] B.K.K. Kasem, S. Jones, Platinum as a Reference Electrode in Electrochemical Measurements, platin met rev 52 (2) (2008) 100–106.

[32] R. Balint, N.J. Cassidy, S.H. Cartmell, Conductive polymers: Towards a smart biomaterial for tissue engineering, Acta Biomaterialia 10 (6) (2014) 2341–2353.

[33] Z. Aqrawe, J. Montgomery, J. Travas-Sejdic, D. Svirskis, Conducting polymers for neuronal microelectrode array recording and stimulation, Sensors and Actuators B: Chemical 257 (2018) 753–765.

[34] A.S. Karimullah, D.R. Cumming, M. Riehle, N. Gadegaard, Development of a conducting polymer cell impedance sensor, Sensors and Actuators B: Chemical 176 (2013) 667–674.

[35] H. Bartsch, R. Peipmann, M. Klett, D. Brauer, A. Schober, J. Müller, PEDOT Coated Thick Film Electrodes for In Situ Detection of Cell Adhesion in Cell Cultures, Biosensors 8 (4) (2018) 105